Optical Detection of Level Crossing in the $(5s5p)\ ^3P_1$ State of Cd^{111} and Cd^{113}†

P. THADDEUS AND R. NOVICK*
Columbia Radiation Laboratory, Columbia University, New York, New York
(Received November 28, 1961; revised manuscript received February 27, 1962)

The magnetic field at which crossing occurs for the $|F,m_F\rangle=|\frac{3}{2},\frac{3}{2}\rangle$ and $|\frac{1}{2},-\frac{1}{2}\rangle$ hyperfine levels of the $(5s5p)\ ^3P_1$ state of Cd^{111} and Cd^{113} has been measured to high precision by observing the change in intensity at an angle of 90° of the resonance fluorescence of the 3261 Å intercombination line. The measured crossing fields, in units of the nuclear magnetic resonance frequency of protons in mineral oil, are $H_c^{111}=8363.408(30)$ kc/sec, $H_c^{113}=8748.734(20)$ kc/sec. Using these results and the known values of the $(5s5p)\ ^3P_1$ hyperfine interval for the two isotopes, we find that the Lánde g_J factor for this state is $g_J^{111}=\frac{3}{2}-160(9)\times10^{-6}$, $g_J^{113}=\frac{3}{2}-146(9)\times10^{-6}$. These results include corrections for second-order interaction with the adjacent fine-structure levels of the $5s5p$ configuration.

INTRODUCTION

THE crossing of levels in a magnetic field may be detected by a change in the angular distribution of resonance fluorescence, as shown by Colegrove, Franken, Lewis, and Sands.[1] Using the 1-μ transition between the $2\ ^3S_1$ and the $2\ ^3P_{0,1,2}$ states of helium, they have succeeded in observing the crossing of several of the Zeeman components of the $2\ ^3P$ states, and have determined the fine structure to high precision.

The level-crossing technique has been extended by Hirsch,[2] and by Dodd[3,4] to the hyperfine levels of the $(6s6p)\ ^3P_1$ state of Hg^{199} and Hg^{201}, while theoretical studies of the effect have been published by Franken,[5] and Rose and Carovillano,[6] following the early work of Breit[7] on resonance fluorescence with partial or complete degeneracy in the excited state. Kibble and Series[8] have studied the line shape of the change in resonance fluorescence at zero magnetic field for the even isotopes of mercury.

As a spectroscopic technique the level-crossing method offers the advantages of experimental simplicity and high resolution. A change in resonance fluorescence is experienced only when the two excited-state levels are separated by an energy of the order of their natural width, typically a small fraction of the Doppler width of the optical transition. This is a resolution usually associated with an optical double-resonance experiment, and in this respect the level-crossing effect may be regarded as a special case of double resonance for which the radio frequency is zero.

Particularly well suited to experiments of this kind are hyperfine levels of the lowest lying $^3P_1$ states of atoms with a $^1S_0$ ground state configuration, such as the alkaline earths, the rare gases, and the group II B metals zinc, cadmium, and mercury. For these elements the intercombination line lies in the ultraviolet, and the natural lifetime of the $^3P_1$ state is usually much longer than that of the $^1P_1$ state of the same configuration due to the close approximation to Russell-Saunders coupling. The hyperfine intervals are typically of the order of a few thousand Mc/sec, and crossings of various Zeeman components will occur in fields of a few kilogauss or less. Mercury, cadmium, and zinc all possess at least one odd isotope, and are especially convenient since they (a) have intercombination lines which do not lie too deeply in the ultraviolet, (b) have the required vapor pressures for maximum fluorescent scattering at much lower temperatures than the alkaline earths, and (c) are much less chemically active than these elements, allowing easy construction of resonance lamps and scattering cells.

For cadmium the lifetime of the $(5s5p)\ ^3P_1$ state is 2.43×10^{-6} sec, and the intercombination line falls at a wavelength of 3261 Å. The naturally occurring odd isotopes Cd^{111} and Cd^{113} each have an abundance of about 12%, and a nuclear spin of $\frac{1}{2}$. The hyperfine interval has been measured for either isotope in a double-resonance experiment.[9] Relevant atomic con-

TABLE I. Atomic constants for Cd^{111} and Cd^{113}.

Isotope	Cd^{111}	Cd^{113}
Fractional abundance	12.75%	12.26%
I	$\frac{1}{2}$	$\frac{1}{2}$
g_I [a]	$+64.80(1)\times10^{-5}$	$+67.78(1)\times10^{-5}$
$\tau(^1P_1)$[b]	$1.59(8)\times10^{-9}$ sec	$1.59(8)\times10^{-9}$ sec
$\tau(^3P_1)$[b,c]	$2.43(10)\times10^{-6}$ sec	$2.43(10)\times10^{-6}$ sec
$\Delta\nu(^3P_1)$[d]	6185.72(2) Mc/sec	6470.79(2) Mc/sec
$\Delta\nu(^3P_2)$[e]	8232.341(2) Mc/sec	8611.586(4) Mc/sec

[a] W. G. Proctor and F. C. Yu, Phys. Rev. **76**, 1728 (1949). Throughout we have followed the convention that the electron g factor is positive.
[b] A. Lurio and R. Novick (to be published).
[c] The value quoted was furnished by F. Byron and M. N. McDermott (private communication).
[d] See reference 9.
[e] W. Faust, M. N. McDermott, and W. Lichten, Phys. Rev. **120**, 469 (1960).

† Work supported in part by a contract with the U. S. Air Force monitored by the Air Force Office of Scientific Research, and in part by a Joint Services Contract with the U. S. Army Signal Corps, the Office of Naval Research, and the Air Force Office of Scientific Research.
* Alfred P. Sloan Foundation Fellow.
[1] F. D. Colegrove, P. A. Franken, R. R. Lewis, and R. H. Sands, Phys. Rev. Letters **3**, 420 (1959).
[2] H. R. Hirsch, Bull. Am. Phys. Soc. **5**, 274 (1960).
[3] J. N. Dodd, Proc. Phys. Soc. (London) **77**, 669 (1961).
[4] J. N. Dodd, Proc. Phys. Soc. (London) **78**, 65 (1961).
[5] P. A. Franken, Phys. Rev. **121**, 508 (1961).
[6] M. E. Rose and R. L. Carovillano, Phys. Rev. **122**, 1185 (1961).
[7] G. Breit, Revs. Modern Phys. **5**, 91 (1933).
[8] B. P. Kibble and G. W. Series, Proc. Phys. Soc. (London) **78**, 70 (1961).
[9] R. F. Lacey (private communication). Preliminary results have appeared in R. F. Lacey, Ph.D. thesis, Massachusetts Institute of Technology, 1959 (unpublished).

TABLE II. The dipole moment matrix connecting the $^3P_1$ state with the $^1S_0$ ground state, evaluated at the crossing point field $H_c \approx -A\,(^3P_1)/\mu_0 g_J$, where g_J is taken as $\frac{3}{2}$. Arbitrary units are used, and states are specified by their low-field quantum numbers.

		$^3P_1$					
	F, m_F	$\frac{3}{2}, \frac{3}{2}$	$\frac{3}{2}, \frac{1}{2}$	$\frac{3}{2}, -\frac{1}{2}$	$\frac{3}{2}, -\frac{3}{2}$	$\frac{1}{2}, \frac{1}{2}$	$\frac{1}{2}, -\frac{1}{2}$
$^1S_0$	$\frac{1}{2}, \frac{1}{2}$	$-(1/2)^{\frac{1}{2}}(\mathbf{i}+i\mathbf{j})$	$0.9291\mathbf{k}$	$(1/3)^{\frac{1}{2}}(\mathbf{i}-i\mathbf{j})$	0	$0.3691\mathbf{k}$	$(1/6)^{\frac{1}{2}}(\mathbf{i}-i\mathbf{j})$
	$\frac{1}{2}, -\frac{1}{2}$	0	$-0.2610(\mathbf{i}+i\mathbf{j})$	$(1/3)^{\frac{1}{2}}\mathbf{k}$	$(1/2)^{\frac{1}{2}}(\mathbf{i}-i\mathbf{j})$	$0.6572(\mathbf{i}+i\mathbf{j})$	$-(2/3)^{\frac{1}{2}}\mathbf{k}$

stants are listed in Table I, while the Zeeman effect of the $^3P_1$ state is shown in Fig. 1. The crossing of the $|F,m_F\rangle = |\frac{3}{2},\frac{3}{2}\rangle$ and $|\frac{1}{2},-\frac{1}{2}\rangle$ levels satisfies, as will be shown in the next section, the requirements of a level-crossing experiment.

THEORY

For transitions from a single ground state $|a\rangle$ to two excited states $|b\rangle$ and $|c\rangle$, which are well separated in energy, Franken[5] obtains for the rate $R(\mathbf{f},\mathbf{g})$, in arbitrary units, at which photons of incoming polarization $\mathbf{f}$ and outgoing polarization $\mathbf{g}$ are scattered:

$$R(\mathbf{f},\mathbf{g}) = R_0 = |f_{ab}|^2 |g_{ba}|^2 + |f_{ac}|^2 |g_{ca}|^2, \tag{1}$$

where $f_{ab} = \langle a|\mathbf{f}\cdot\mathbf{r}|b\rangle$, etc.

In the vicinity of crossing

$$R(\mathbf{f},\mathbf{g}) = R_0 + \frac{A+A^*}{1+4\pi^2\tau^2\nu^2(b,c)} + \frac{(A-A^*)2\pi i\tau\nu(b,c)}{1+4\pi^2\tau^2\nu^2(b,c)}, \tag{2}$$

where $A = f_{ba}f_{ac}g_{ca}g_{ab}$, τ is the mean lifetime of each excited state, and $\nu(b,c) = (E_b - E_c)/h$.

When A is real, the change in resonance fluorescence S produced by the crossing has a Lorentzian line shape with a full half-width $\Delta\nu(b,c) = 1/\pi\tau$, while when A is pure imaginary the effect has a dispersion-type line shape, and in the general case of A complex, a mixture of these two profiles.

It is evident that crossing of Zeeman levels of different hyperfine states occurs when the Zeeman energy is comparable to the hyperfine energy, so that the mixing of states of different F, but the same m_F may be considerable. Using the hyperfine Hamiltonian,

$$\mathcal{H} = A\,(^3P_1)\mathbf{I}\cdot\mathbf{J} + g_J\mu_0 J_z H + g_I\mu_0 I_z H, \tag{3}$$

for the $^3P_1$ state of Cd^{111} and Cd^{113}, the crossing of the levels $|b\rangle$ and $|c\rangle$ (Fig. 1) may be shown to take place in a field H_c such that

$$g_J = -A\,(^3P_1)/\mu_0 H_c - \tfrac{1}{2}g_I. \tag{4}$$

In terms of the low-field states $|F,m_F\rangle$, $|c\rangle = |\frac{3}{2},\frac{3}{2}\rangle$ for all field values, while the composition of $|b\rangle$ at the crossing field H_c is, if we neglect the small contribution of g_I in Eq. (4),

$$|b\rangle = (2\sqrt{2}/3)|\tfrac{1}{2},-\tfrac{1}{2}\rangle - \tfrac{1}{3}|\tfrac{3}{2},-\tfrac{1}{2}\rangle. \tag{5}$$

The dipole-moment matrix in this intermediate representation connecting the various hyperfine levels of the $^3P_1$ state with the $^1S_0$ ground state of the atom is given in Table II. From this matrix we can derive (a) the most convenient geometrical arrangement for the experiment, (b) the line shape as a function of the angle between the incoming and scattered light, and (c) the magnitude of the effect.

(a) Since neither states $|b\rangle$ nor $|c\rangle$ are connected to the ground state $|a\rangle = |^1S_0,\frac{1}{2},\frac{1}{2}\rangle$ by a photon polarized along the direction of the magnetic field (z axis), we are free, without loss of generality, to design the experiment with the incoming and scattered photons polarized and propagating in the transverse (xy) plane. The outgoing photon is then specified uniquely by the angle θ between its direction of polarization and the direction of polarization of the incident photon (which we will take as the x axis).

(b) The matrix elements of $\mathbf{f}$ and $\mathbf{g}$ then become, in the units of Table II,

$$\begin{aligned} f_{ab} &= (1/6)^{\frac{1}{2}}, \quad & g_{ab} &= (1/6)^{\frac{1}{2}}(\cos\theta - i\sin\theta), \\ f_{ac} &= -(1/2)^{\frac{1}{2}}, \quad & g_{ac} &= -(1/2)^{\frac{1}{2}}(\cos\theta + i\sin\theta), \end{aligned} \tag{6}$$

and

$$A = (1/12)[\cos(2\theta) - i\sin(2\theta)]. \tag{6a}$$

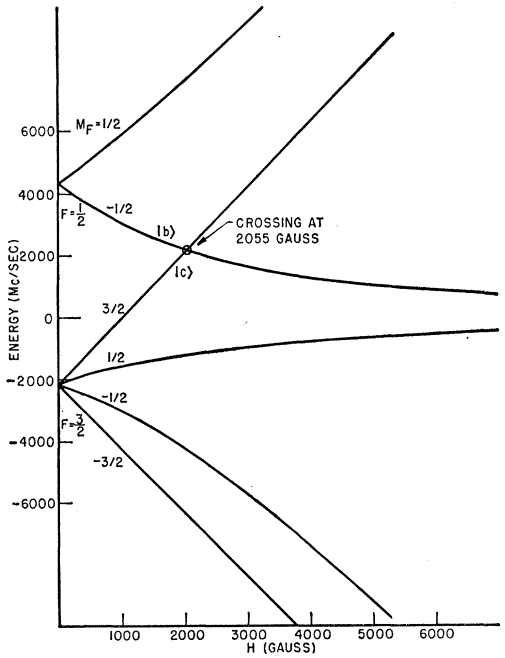

FIG. 1. Zeeman effect of the hyperfine structure of the $(5s5p)\ ^3P_1$ state of Cd^{113}. The crossing point for Cd^{111} occurs near 1964 gauss.

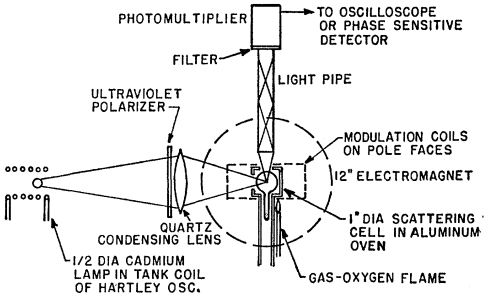

FIG. 2. Schematic illustration of the experimental apparatus.

Thus at $\theta=0$, 90° we expect a pure Lorentzian, while at $\theta=45°$ a pure dispersion-type line shape. For the linewidth at 90°,

$$\Delta H=(dH/d\nu(b,c))_{H_c}(1/\pi\tau)$$
$$=45 \text{ mgauss, in the present case.}$$

An idea of the sharpness of the effect may be obtained using Eq. (4):

$$\Delta H/H=45 \text{ mgauss}\times\mu_0 g_J/A(^3P_1)\approx 1/20\,000.$$

(c) Assuming that the scattering angle is 90°, and that the light from the resonance lamp used has a linewidth much larger than the hyperfine structure, the fractional change in the fluorescence at the crossing point is, for a single isotope, and considering all possible hyperfine transitions from the ground to the excited state for an incident x and scattered y or z photon,

$$S/R_0'=(A+A^*)/R_0'=2A/R_0', \tag{7}$$

where, from Table II,

$$R_0'=\sum_{m,m',m''}|f_{mm'}|^2|g_{m'm''}|^2=7/6,$$

giving

$$S/R_0'=1/7. \tag{7a}$$

Besides being quite sharp, the crossing-point effect is seen to be relatively large.

DESCRIPTION OF THE EXPERIMENT

A schematic illustration of the experiment is shown in Fig. 2. Light from an electrodeless rf cadmium resonance lamp was passed through an ultraviolet polarizer, and focussed by a quartz lens onto a scattering cell which lay between the poles of a 12-in. electromagnet. 3261 Å light scattered at right angles was observed using a DuMont K 1306 ultraviolet photomultiplier tube. A Schott UG-11 filter effectively excluded other lines produced by the lamp, in particular, the 2288 Å, $^1P_1-{}^1S_0$ resonance transition, which is strongly scattered by the atomic vapor. To remove the photomultiplier from the magnetic field without sacrificing solid angle, a light pipe was used consisting of three feet of glass tubing aluminized on the inside.

The lamps used during this experiment gave about a watt of power (over 4π solid angle) at 3261 Å without self reversal. They consisted of a small sphere of quartz about $\frac{1}{2}$ in. in diameter, which had been baked at 1000°C for about half a day, and purged using an intense argon discharge for several hours, before being loaded with a small quantity of distilled cadmium, and about 1 mm Hg of spectroscopically pure argon. A lamp prepared in this way was found to run for many hours before the walls were discolored, or the discharge quenched by impurities driven from the walls. The lamp was excited by placing it within the tank coil of a strongly driven Hartley oscillator which operated in the region of 30 Mc/sec. Optimum lamp output was found to depend rather critically on the oscillator level.

The two scattering cells used were about an inch in diameter, and were prepared like the lamps, but were sealed off, without the addition of argon, at a pressure of typically 10^{-7} mm Hg. They had a thin tubular extension about 2 in. long at the bottom which was maintained at a slightly lower temperature than the rest of the cell, and determined the cadmium vapor pressure. The cell could be heated to at least 400°C by a single gas-oxygen flame which played on the outside of the oven. Temperature measurements were made with a thermocouple near the top of the cell, and do not therefore accurately reflect the true temperature of the cadmium reservoir.

To reduce instrumental scattering, the cell and oven were thoroughly blackened with a smoky acetylene flame, and small entrance and exit windows wiped on the quartz surfaces.

The photomultiplier current as a function of temperature for a magnetic field near 2000 gauss is shown in Fig. 3. It can be seen that instrumental scattering was small compared to fluorescent scattering above 200°C, while above 300°C the vapor pressure was so great that multiple scattering reduced the light reaching the photomultiplier.

This preliminary measurement of fluorescence allowed an estimate, on the basis of shot noise in the photomultiplier, to be made of the expected signal-to-noise

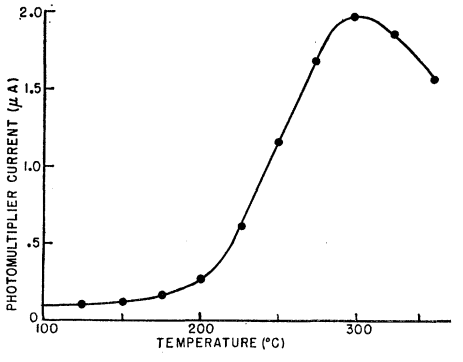

FIG. 3. Scattered power at an angle of 90° as a function of the cell temperature for a magnetic field near 2000 gauss.

ratio of the crossing effect. Using Eq. (7a),

$$\text{signal/noise} = (f/7)(i/2eGB)^{\frac{1}{2}} \approx 4, \qquad (8)$$

where e is the electronic charge, $f \approx 0.12$ is the fractional isotopic abundance, $G \approx 7\times10^4$ is the photomultiplier gain, $B \approx 1000$ cps is the approximate detector bandwidth for the oscilloscope display used, and $i \approx 1.7\times10^{-6}$ amp from Fig. 3.

EXPERIMENTAL RESULTS

The signal strength of the observed crossings, as shown in Fig. 4, agreed closely with the estimate given by Eq. (8). The line width is about twice that expected on the basis of the lifetime of the $^3P_1$ state, due presumably to field inhomogeneities over the sample. Field modulation at 30 cps was provided by rectangular coils attached to the magnet pole faces. In Fig. 5 are shown the signals obtained with narrow-band, phase-sensitive detection at the same modulation frequency, with an effective detector bandwidth of less than 1 cps, and at various scattering angles.

Measurements of the crossing field to an accuracy of better than one part in 10^5 were made with a small mineral-oil nuclear-magnetic-resonance probe, placed as close to the oven as possible, the proton resonance pip being superimposed on the crossing signal using a dual-beam oscilloscope, and the nuclear resonance oscillator frequency being read on a Hewlett-Packard Model 524C direct-reading frequency counter. To measure the slight differential field, of the order of one part in 10^4, between the probe and the scattering cell, a second, larger mineral-oil probe was constructed that approximated the cell in size, and could be placed accurately in the cell position. This was driven by a second oscillator, the two nuclear-resonance pips then being superimposed on the dual-beam oscilloscope, and the beat frequency measured by the counter. This scheme was quite flexible and had the virtue that no inaccuracies due to drifts in the magnet current, typically of the order of a part in 10^5 over a few seconds, were introduced.

The crossing was measured using the relatively weak signals obtained with oscilloscope display, rather than the strong narrow-band detector signals, primarily to avoid errors due to these long-term field fluctuations. Prior to a run, however, to ensure that the effective angle was exactly 90° and no admixture of the dispersion-type profile shifted the signal peak, the angles were adjusted so that the derivative curve in Fig. 5(a)

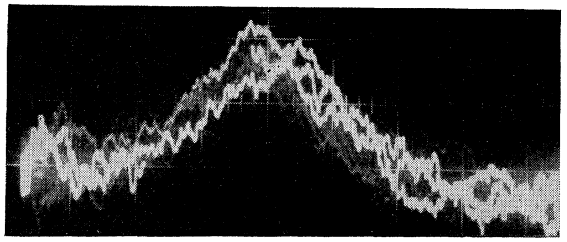

(a)

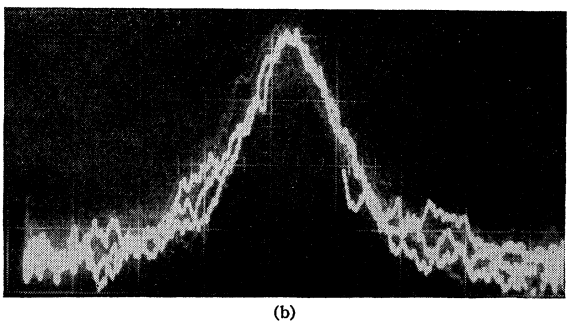

(b)

FIG. 4. Oscilloscope traces of the crossing point effect for (a) Cd^{111} and (b) Cd^{113}, using 30-cps field modulation. The linewidth in either case is about 125 mgauss. The Cd^{113} crossing point was consistently observed to be about twice as strong as that for Cd^{111}, due presumably to the isotope shift of the $^3P_1-{}^1S_0$ transition, and greater lamp output at the exact Cd^{113} wavelength.

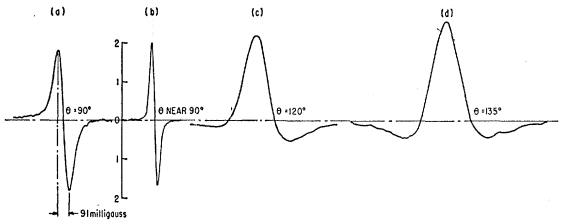

FIG. 5. Recorder traces of the crossing point effect for Cd^{113}, using phase-sensitive detection at 30 cps, with time constants of about 1 sec. The signal shown is the derivative of the true line shape, providing the field modulation is sufficiently small. In (a) the incoming and scattered light cones have been adjusted to give an effective scattering angle of 90°, and the upper and lower peaks are of equal size, while in (b) the lower half of the incoming light cone has been blocked out to give an effective scattering angle greater than 90°, with a consequent slight admixture of the dispersion-type line shape, and an asymmetry of the observed derivative. In (c) the scattering angle is 120° and in (d) 135°, where the signal is the derivative of a pure dispersion-type curve. The various apparent linewidths shown are due to different field-sweep rates.

TABLE III. The measured values of the crossing-point fields in units of the nuclear magnetic resonance frequency of protons in mineral oil. To reduce systematic errors, following run II the large proton probe was dismantled and again assembled to approximate the cell position. The uncertainties given for each run are standard deviations, while the uncertainty in the final averages includes an estimated contribution of 15 cps for possible systematic errors.[a]

	Cd^{111}		Cd^{113}	
	Crossing field (kc/sec)	Number of readings	Crossing field (kc/sec)	Number of readings
Run I	8363.440(9)	10	8748.725(15)	18
	8363.384(11)	10	8748.722(11)	10
			8748.725(8)	10
Run II	8363.379(12)	10	8748.748(14)	10
			8748.741(10)	10
Run III	8363.427(7)	16	8748.730(9)	8
	8363.409(8)	8	8748.746(5)	16
Average	8363.408(30)		8748.734(20)	

[a] Preliminary results have appeared in Bull. Am. Phys. Soc. **6**, 74 (1961); **5**, 411 (1960).

TABLE IV. The matrix elements of the hyperfine Hamiltonian including second-order corrections relevant to the crossing of the levels $|b\rangle$ and $|c\rangle$, in the representation $|F,m_F\rangle$.

$$\langle \tfrac{3}{2},\tfrac{3}{2}|\mathcal{H}|\tfrac{3}{2},\tfrac{3}{2}\rangle=\tfrac{1}{2}A(^3P_1)+(g_J+\tfrac{1}{2}g_I)\mu_0H-\frac{\alpha^2}{4}\frac{\mu_0^2H^2}{\delta_2}-\frac{\sqrt{3}\alpha}{8}\left[c_1a_s-\left(c_1+c_2\frac{5\sqrt{2}\xi}{8}\right)a_{\frac{3}{2}}\right]\frac{\mu_0H}{\delta_2}$$
$$-\frac{\alpha^2\beta^2}{4}\frac{\mu_0^2H^2}{\delta_1}+\frac{\alpha\beta}{8}\left[-3c_1c_2a_s+5\left(c_1c_2+\frac{c_1^2-c_2^2}{4\sqrt{2}}\xi\right)a_{\frac{3}{2}}-2c_1c_2a_{\frac{1}{2}}\right]\frac{\mu_0H}{\delta_1}$$

$$\langle \tfrac{3}{2},-\tfrac{1}{2}|\mathcal{H}|\tfrac{3}{2},-\tfrac{1}{2}\rangle=\tfrac{1}{2}A(^3P_1)-(\tfrac{1}{3}g_J+\tfrac{1}{6}g_I)\mu_0H+\frac{4\alpha^2}{9}\frac{\mu_0^2H^2}{\delta_0}-\frac{11\alpha^2}{36}\frac{\mu_0^2H^2}{\delta_2}+\frac{\sqrt{3}\alpha}{24}\left[c_1a_s-\left(c_1+c_2\frac{5\sqrt{2}\xi}{8}\right)a_{\frac{3}{2}}\right]\frac{\mu_0H}{\delta_2}$$
$$-\frac{\alpha^2\beta^2}{12}\frac{\mu_0^2H^2}{\delta_1}-\frac{\alpha\beta}{24}\left[-3c_1c_2a_s+5\left(c_1c_2+\frac{c_1^2-c_2^2}{4\sqrt{2}}\xi\right)a_{\frac{3}{2}}-2c_1c_2a_{\frac{1}{2}}\right]\frac{\mu_0H}{\delta_1}$$

$$\langle \tfrac{1}{2},-\tfrac{1}{2}|\mathcal{H}|\tfrac{1}{2},-\tfrac{1}{2}\rangle=-A(^3P_1)-(\tfrac{2}{3}g_J-\tfrac{1}{6}g_I)\mu_0H+\frac{2\alpha^2}{9}\frac{\mu_0^2H^2}{\delta_0}-\frac{\alpha}{(6)^{\frac{1}{2}}}\left[c_2(a_s-a_{\frac{1}{2}})-c_1\frac{5\sqrt{2}\xi}{8}a_{\frac{3}{2}}\right]\frac{\mu_0H}{\delta_0}-\frac{5\alpha^2}{18}\frac{\mu_0^2H^2}{\delta_2}$$
$$-\frac{\alpha^2\beta^2}{6}\frac{\mu_0^2H^2}{\delta_1}+\frac{\alpha\beta}{6}\left[-3c_1c_2a_s+5\left(c_1c_2+\frac{c_1^2-c_2^2}{4\sqrt{2}}\xi\right)a_{\frac{3}{2}}-2c_1c_2a_{\frac{1}{2}}\right]\frac{\mu_0H}{\delta_1}$$

$$\langle \tfrac{3}{2},-\tfrac{1}{2}|\mathcal{H}|\tfrac{1}{2},-\tfrac{1}{2}\rangle=-\frac{\sqrt{2}}{3}(g_J-g_I)\mu_0H-\frac{2\sqrt{2}\alpha^2}{9}\frac{\mu_0^2H^2}{\delta_0}+\frac{\sqrt{3}\alpha}{6}\left[c_2(a_s-a_{\frac{1}{2}})-c_1\frac{5\sqrt{2}\xi}{8}a_{\frac{3}{2}}\right]\frac{\mu_0H}{\delta_0}+\frac{\sqrt{2}\alpha^2}{36}\frac{\mu_0^2H^2}{\delta_2}$$
$$-\frac{5\alpha}{8(6)^{\frac{1}{2}}}\left[c_1a_s-\left(c_1+c_2\frac{5\sqrt{2}\xi}{8}\right)a_{\frac{3}{2}}\right]\frac{\mu_0H}{\delta_2}-\frac{\sqrt{2}\alpha^2\beta^2}{12}\frac{\mu_0^2H^2}{\delta_1}$$
$$+\frac{\sqrt{2}\alpha\beta}{48}\left[-3c_1c_2a_s+5\left(c_1c_2+\frac{c_1^2-c_2^2}{4\sqrt{2}}\xi\right)a_{\frac{3}{2}}-2c_1c_2a_{\frac{1}{2}}\right]\frac{\mu_0H}{\delta_1}$$

was exactly symmetrical, and the signal a pure Lorentzian. The results of the crossing field measurements are summarized in Table III.

SECOND-ORDER CORRECTIONS TO g_J

Due to the high precision with which the $^3P_1$ hyperfine interval is known for both Cd^{111} and Cd^{113} (Table I), the primary value of the present experiment lies in a determination for this state of g_J to comparable accuracy. Equation (4) for g_J, however, does not take into account terms in the hyperfine and Zeeman energies off-diagonal in J, which are expected to contribute to g_J corrections of the order of the ratio of the hyperfine to fine structure energies, or about one part in 10^4, more than ten times that produced by the uncertainty in H_c. For mercury, Dodd[3] has derived an expression for the corrections due to the Zeeman terms off-diagonal in J, but has neglected similar terms in the hyperfine interaction which are of the same magnitude.

Our procedure for calculating these terms may be summed up as follows[10]: We have evaluated the hyperfine and Zeeman interactions for the p and s valance electrons in a representation $|j_1j_2Jm_J\rangle$ following the relativistic treatment of Schwartz.[11,12] This Hamiltonian involves four hyperfine constants, a_s, $a_{\frac{3}{2}}$, $a_{\frac{1}{2}}$, and ξ, in his notation. The ratio $a_{\frac{3}{2}}/a_{\frac{1}{2}}$, however, reduces to the ratio of radial integrals of the solution of the single particle Dirac equation, and is calculated by Schwartz[11] for an $l=1$ electron. For cadmium we obtain $a_{\frac{1}{2}}=6.42a_{\frac{3}{2}}$. ξ is a

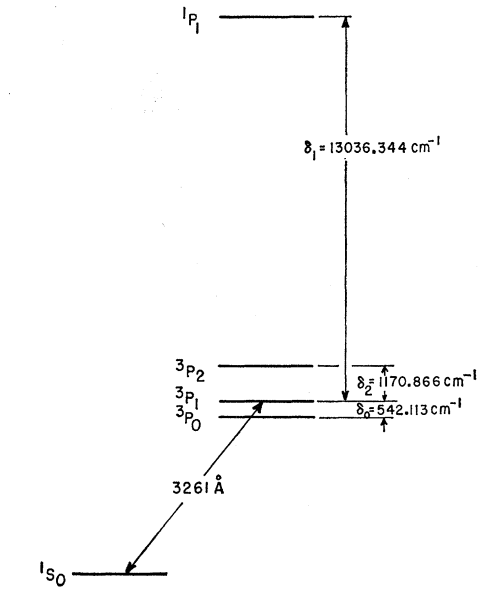

FIG. 6. Fine structure of the $(5s5p)$ cadmium configuration.

[10] A. Lurio, R. Novick, and M. Mandel, this issue [Phys. Rev. **126**, 1758 (1961)].
[11] C. Schwartz, Phys. Rev. **97**, 380 (1955).
[12] C. Schwartz, Phys. Rev. **105**, 173 (1957).

TABLE V. The hyperfine coupling constants and second-order correction terms, calculated from Eq. (12) and the lifetime and hyperfine intervals given in Table I.

Isotope	Cd^{111}	Cd^{113}
a_s (kMc/sec)	−12.354(33)	−12.923(35)
$a_{\frac{1}{2}}$ (kMc/sec)	−1.752(71)	−1.833(75)
$a_{\frac{3}{2}}$ (kMc/sec)	−0.273(11)	−0.285(12)
$+[(3)^{\frac{1}{2}}\alpha/6]\{c_1a_s-[c_1+c_2(5\sqrt{2}\xi/8)]a_{\frac{1}{2}}\}(1/\delta_2)$	$-52.0(3)\times10^{-6}$	$-54.4(3)\times10^{-6}$
$+(\alpha^2\mu_0H_c/24)[(8/\delta_0)-(1/\delta_2)]$	$+53.0(1)\times10^{-6}$	$+55.5(1)\times10^{-6}$
$-[(6)^{\frac{1}{2}}\alpha/6][c_2(a_s-a_{\frac{1}{2}})-c_1(5\sqrt{2}\xi/8)a_{\frac{1}{2}}](1/\delta_0)$	$+220.4(20)\times10^{-6}$	$+230.5(20)\times10^{-6}$
Total correction	$+221.4(24)\times10^{-6}$	$+231.6(24)\times10^{-6}$

second-order correction of the order of unity, estimated to be

$$\xi=+[1+3\alpha^2Z^2/2l(l+1)n^*]^{\frac{1}{2}}G/F_{\frac{3}{2}}, \quad (9)$$

where n^* is the effective quantum number of the $^3P_1$ state, and the relativistic correction factors G and $F_{\frac{3}{2}}$ for an $l=1$ electron are also given in Fig. 1 of reference 11, and in Kopfermann.[13] Only two independent hyperfine constants remain, which ultimately are determined from the known $^3P_2$ and $^3P_1$ hyperfine intervals.

The diagonalization of this Hamiltonian is most conveniently accomplished in two operations. Initially, a transformation is made from the jj coupling scheme into the nearly LS representation which applies to the fine structure of the $5s5p$ configuration, shown in Fig. 6. As is well known, the fine-structure intervals are not a reliable indication of the exact degree of intermediate coupling due to spin-spin, spin-other-orbit, etc. fine-structure interactions in addition to the spin-orbit interaction mainly responsible for the breakdown of LS coupling.[14] The lifetimes of the $^1P_1$ and $^3P_1$ states are reasonably well known for cadmium, however (Table I), and give a direct measure of the mixture of the two states. If we write for the nominally $^3P_1$ state

$$\psi=\alpha|^3P_1\rangle+\beta|^1P_1\rangle, \quad (10)$$

then

$$\frac{\beta^2}{\alpha^2}=\frac{\tau(^1P_1)}{\tau(^3P_1)}\frac{\lambda^3(^3P_1-^1S_0)}{\lambda^3(^1P_1-^1S_0)}=(1.89\pm0.10)\times10^{-3}, \quad (11)$$

and $\alpha=0.99906(5)$, $\beta=-0.0434(23)$ while the c coefficients which transform from the jj representation are[10]: $c_1=(1/3)^{\frac{1}{2}}\alpha+(2/3)^{\frac{1}{2}}\beta=0.5414(20)$, $c_2=(2/3)^{\frac{1}{2}}\alpha-(1/3)^{\frac{1}{2}}\beta=0.8408(13)$. The uncertainties in these coefficients arise from the experimental uncertainties in the determination of the lifetimes (see Table I). It is reassuring to note that we obtain $\beta^2/\alpha^2=2.22\times10^{-3}$ from the observed fine structure when we include the correction for the spin-other-orbit interaction (Wolfe correction). However, since we believe the lifetime method to be more reliable we will use the result given by Eq. (11) when estimating the second-order corrections.

With the Hamiltonian in this representation, terms off-diagonal in J may be treated as a perturbation on the diagonal terms, most conveniently using the transformation method of Van Vleck.[15] The final matrix elements relevant to the levels $|b\rangle$ and $|c\rangle$ are given in Table IV. When the quadratic secular equation is solved, and the energies of states $|b\rangle$ and $|c\rangle$ equated, we find that

$$g_J=\frac{g_pA(^3P_1)}{h\nu_p}-\frac{g_I}{2}+\frac{\alpha^2\mu_0H_c}{24}\left(\frac{8}{\delta_0}+\frac{3\beta^2}{\delta_1}-\frac{1}{\delta_2}\right)$$
$$-\frac{(6)^{\frac{1}{2}}\alpha}{6}\left[c_2(a_s-a_{\frac{1}{2}})-c_1\frac{5\sqrt{2}\xi}{8}a_{\frac{1}{2}}\right]\frac{1}{\delta_0}$$
$$+\frac{(3)^{\frac{1}{2}}\alpha}{6}\left[c_1a_s-\left(c_1+c_2\frac{5\sqrt{2}\xi}{8}\right)a_{\frac{1}{2}}\right]\frac{1}{\delta_2}, \quad (12)$$

where g_p is the proton g factor, ν_p the nuclear magnetic resonance frequency of protons at the crossing field, α and β the mixing coefficient given above, and δ_0, δ_1 and δ_2 are the magnitude of the fine structure separations shown in Fig. 6. The term arising from the interaction with the $^1P_1$ state contributes less than one part in 10^7 to the final value of g_J. In Eq. (12) and Table IV, all field-independent terms involving the square of the hyperfine constants following the Van Vleck transformation have been absorbed into A ($^3P_1$). At low magnetic fields, such as in a double-resonance experiment, this is therefore the directly measured $\mathbf{I}\cdot\mathbf{J}$ constant. The terms in $8/\delta_0$ and $1/\delta_2$ proportional to H_c of Eq. (12) are identical with Dodd's Zeeman corrections.[3]

The numerical values of the hyperfine coupling constants as determined from the intervals in the $^3P_1$ and $^3P_2$ states, and the second-order correction terms, are listed in Table V. Using the recent value 1/657.462(3) reported by Liebes and Franken[16] for $g_p/2$ in mineral oil, g_J is calculated as

$$g_J^{111}=\tfrac{3}{2}-160(9)\times10^{-6},$$
$$g_J^{113}=\tfrac{3}{2}-146(9)\times10^{-6}.$$

The difference between these results is not believed to be significant.

[13] H. Kopfermann, *Nuclear Moments* (Academic Press Inc., New York, 1958), Table VIII.
[14] G. Araki, Progr. Theoret. Phys. (Kyoto) **3**, 262 (1948).
[15] E. C. Kemble, *Fundamental Principles of Quantum Mechanics* (McGraw-Hill Book Company, Inc., New York, 1937), p. 394.
[16] S. Liebes and P. Franken, Phys. Rev. **116**, 633 (1959).

A theoretical estimate of g_J exclusive of relativistic and diamagnetic effects is given by

$$g_J=\tfrac{1}{2}\alpha^2(g_L+g_S)+\beta^2 g_L, \tag{13}$$

where α and β are again the mixing coefficients of Eq. (10).

Using $g_L=1-m/M$ and $g_S=2(1.0011596)$, we find

$$g_J=\tfrac{3}{2}-\tfrac{1}{2}\beta^2+\alpha^2(0.0011596)-\tfrac{1}{2}(m/M).$$

Applying this formula to cadmium, we obtain

$$g_J=\tfrac{3}{2}-18(80)\times 10^{-6}.$$

The uncertainty in this result arises almost entirely from the uncertainty in β.

By comparing this result with the mean of the experimental values, we find that the relativistic and diamagnetic corrections are

$$\Delta g_{\text{rel}}+\Delta g_{\text{diam}}=-135(81)\times 10^{-6},$$

a figure not unreasonable in the light of previous estimates[17,18] for other atoms. Theoretical calculations of these corrections for cadmium and other group II elements are in progress and will be reported in a later publication.

ACKNOWLEDGMENTS

We are indebted to the staff of the Columbia Radiation Laboratory, and in particular to C. Dechert and A. Deery for their assistance during the course of this work. Discussions with Professor P. Franken and Professor H. Foley are gratefully acknowledged, as are the services of A. Landman, who checked many of the calculations.

---

[17] A. Abragam and J. H. Van Vleck, Phys. Rev. **92**, 1448 (1953).
[18] A. Lurio, G. Weinreich, C. W. Drake, V. W. Hughes, and J. A. White, Phys. Rev. **120**, 153 (1960).

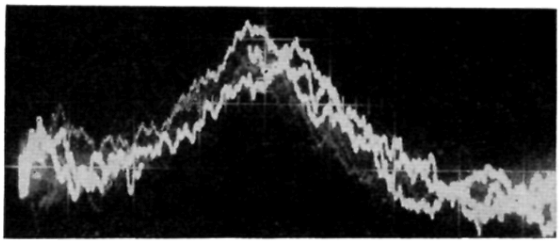

(a)

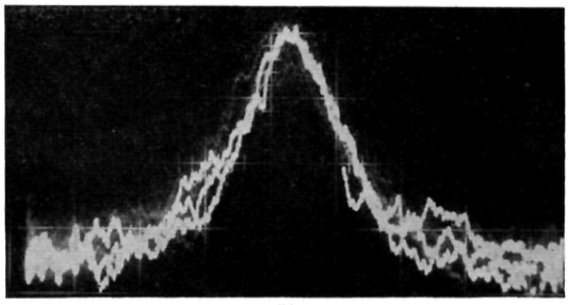

(b)

FIG. 4. Oscilloscope traces of the crossing point effect for (a) Cd^{111} and (b) Cd^{113}, using 30-cps field modulation. The linewidth in either case is about 125 mgauss. The Cd^{113} crossing point was consistently observed to be about twice as strong as that for Cd^{111}, due presumably to the isotope shift of the $^3P_1-{}^1S_0$ transition, and greater lamp output at the exact Cd^{113} wavelength.